Secondary electrons induced by fast ions under channeling conditions. I. Production and emission of secondary electrons

Hiroshi Kudo and Kunihiro Shima
Institute of Applied Physics, University of Tsukuba, Ibaraki 305, Japan

Kohzoh Masuda
Institute of Materials Science, University of Tsukuba, Ibaraki 305, Japan

Seiji Seki*
Tandem Accelerator Center, University of Tsukuba, Ibaraki 305, Japan
(Received 20 February 1990; revised manuscript received 22 October 1990)

Energy spectra of ion-induced secondary electrons emitted from Si and GaAs single crystals have been measured for various ions with a velocity of 3.75 MeV/amu. A simple Z_1^2-scaling behavior of the electron yields indicates that the observed keV electrons stem from simple binary collisions between the ions and the target electrons. Measurements for GaAs crystals preamorphized with 2-keV Ar^+ ions provide evidence for the localization of the binary collisions near the surface region under channeling incidence conditions. Furthermore, these measurements are used to determine the effective target thicknesses both for channeling and random incidence conditions.

I. INTRODUCTION

Magnuson and Carlston[1] observed that in experiments using Ar^+ beams (in the range of 0.5–10 keV) the ion-induced emission of secondary electrons from single-crystal targets depends strongly on the incident direction of the ions. Similarly, by using medium-energy (less than 100 keV) ions several authors have found that the reduction of the total electron yield under channeling incidence conditions reflects the orientation of the atomic rows or planes with respect to the ion-beam direction.[2–4] General trends in those observations, e.g., the strong reduction of the electron yield under major axial channeling conditions, can be qualitatively understood in terms of the well-known ion-beam shadowing effect.

For a better understanding of this shadowing phenomenon, the energy spectra of the electrons emitted under channeling incidence conditions must be analyzed. Such energy spectra for fast ions in the MeV/amu range have been already measured by MacDonald *et al.*,[5] Kudo *et al.*,[6–8] and Wong *et al.*[9] but with a particular interest in the emission of target Auger electrons. Under channeling incidence conditions, the electron yields reported in those papers exhibit a marked decrease in the high-energy region (above a few keV), compared with random (nonchanneling) cases. Recent measurements by Kudo *et al.*[10] using various 2–8-MeV/amu ions have shown that the reduction in the electron yield under channeling incidence conditions can be interpreted as a decrease in the effective target thickness, resulting from the ion-beam shadowing effect.

The observation of shadowing using secondary electrons could possibly provide applications to the study of particle-solid interactions, since information obtainable by this method includes the ion's behavior at large distances from the atomic rows. Actually, even in a large impact parameter collision between an ion and a target atom, the outer-shell or valence electrons can be scattered by the ion and contribute to the observed electron yields. This is in contrast to the case of Rutherford backscattering analysis or characteristic x-ray spectroscopy under channeling conditions,[11] where information obtained is rather restricted to close-impact collisions.

For such an application of the shadowing effect, more fundamental studies of the emission of secondary electrons are necessary. In fact, analyses of experimental data requires knowledge on the mechanism of the production of secondary keV electrons. This mechanism, which can be inferred from the dependence of electron yield on the atomic number of the ions, must be experimentally elucidated prior to extended studies of the shadowing effect.

The localization of the projectile-electron collisions near the surface under channeling incidence conditions has been confirmed previously by an observed scaling characteristic of the shadowing effect.[10] Also, measurements of the localized-collision effect using damaged crystals, for which the displaced atoms should enlarge the effective target thickness may provide information useful for the interpretation of the reduced electron yield under channeling incidence conditions.

This paper describes the processes of the production and emission of high-energy secondary electrons in damaged or undamaged single crystals under channeling or random incidence conditions.

II. EXPERIMENTAL

Collimation of the ion beam is important for the collection of the energy spectra of secondary electrons under well-defined beam conditions. As shown in Fig. 1, the ion

 ©1991 The American Physical Society

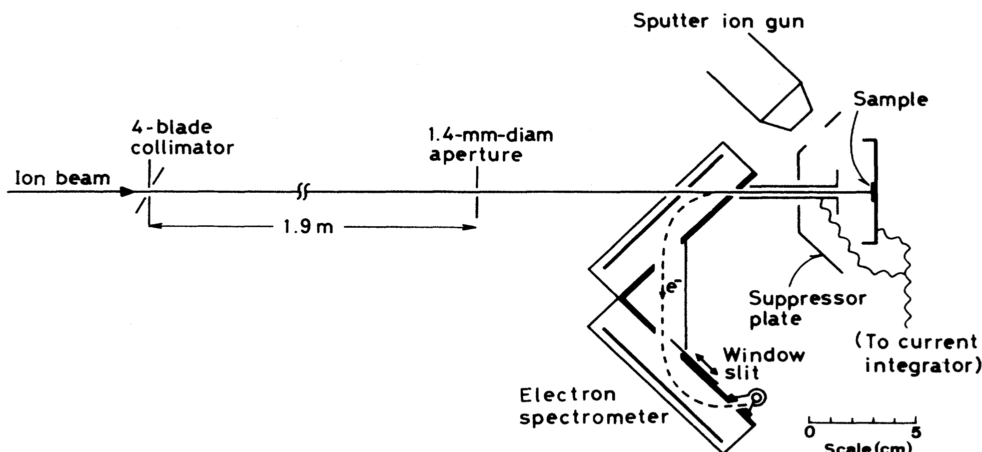

FIG. 1. Schematic diagram of the experimental arrangement.

beam first passes through a remotely controlled 4-blade collimator, a 1.4-mm-diameter aperture, a 3-mm-diameter beam path within a spectrometer, and subsequently impinges on a target crystal. To avoid beam scattering and emission of secondary electrons at the edge of the aperture, the 4-blade collimator was symmetrically narrowed so that the beam current on target was reduced to 20–30% of the maximal attainable current. The resulting beam size on the target is about 0.6×0.6 mm^2, appreciably smaller than the aperture.

To prevent the electrons emitted at 180° from being decelerated by the electric field around the suppressor plate (-200 V), an aluminum guide pipe with a disk on its end was mounted between the sample and the entrance of the spectrometer, and was connected to the beam current integrator, as shown in Fig. 1. The beam current was thus accurately measured by merging the pipe current with the sample current.[7,10]

The angular divergence of the incident ion beam was sufficiently less than the critical angles for channeling, i.e., 1 –5 mrad for our experiments. This was confirmed by the fact that the ratio of the channeling to random yield remained unchanged when the beams were more tightly collimated, which geometrically restricted the beam divergence to less than the critical angles noted above. This fact also assured proper beam transport conditions down to the 4-blade collimator. In fact, the beam divergence was less than that defined by the collimator and the aperture.

When the target crystals were bombarded with MeV/amu light ions (especially deuterons), γ rays emitted from the target impinged on the electron multiplier (Ceratron) and produced uniform backgrounds in the electron spectra. Those backgrounds were, however, easily measured independently by closing the window slit of the spectrometer, shown in Fig. 1, which ensured counting of only γ-ray signals. The uniform backgrounds, which depended on the incident (channeling or random) conditions, were subtracted from the spectra.

The crystals used are chemically etched Si(110), Si(100), and GaAs (100) wafers. An Ar sputter ion gun, shown in Fig. 1, was used to produce lattice disorder in the surface region of the samples. Other experimental details, for example, the operation of the electron spectrometer, have been described elsewhere.[10]

The measurements were carried out at 290–295 K and a pressure of about 3×10^{-6} Pa. The ion beams were obtained from the Pelletron Tandem Accelerator at the University of Tsukuba. The beam current on target was 5–10 nA for all of the ions used.

III. RESULTS AND DISCUSSION

The energy spectra of the secondary electrons presented here are raw data from which the uniform γ-ray background, when present, has been subtracted.

A. Secondary electrons produced by close-encounter collisions

Figure 2 shows energy spectra of the secondary electrons induced by 3.75-MeV/amu $^{2}H^{+}$ (deuterons), $^{4}He^{2+}$, $^{28}Si^{13+}$, and $^{35}Cl^{11+}$ for random incidences on Si crystals. The electron yields for the same number of the incident ions are normalized to the square of the atomic numbers, Z_1, of the ions. In this case, the binary-peak energy, i.e., the maximum energy transferable from an ion to a free electron at rest, is 8.2 keV. Therefore, the spectra shown in Fig. 2 cover most of the spectrum range to which both inner-shell and valence electrons contribute. The charge state of the incident ions affects the electron yield only near or below the loss-peak energy, 2 keV in this case, as reported previously for C and O ions[10] and recently also confirmed for Si (Si^{13+} and Si^{14+}) and S (S^{10+} and S^{15+}) ions.

Figure 2 demonstrates a simple Z_1^2-scaling behavior of the electron yield at electron energies above about 2 keV, within an estimated uncertainty of 20% in the vertical

scale in spite of the wide variation of Z_1^2 from 1 (for ^{2}H) to 289 (for Cl). The 20% uncertainty originates from a slightly different setting of the 4-blade collimator and the window slit (about 5 mm wide) for transporting different ions, which affects the focusing conditions of the analyzed electrons into the electron multiplier and accordingly gives rise to a change in the counting efficiency. Actually, a similar difference in the electron yield was observed when the beam collimation was changed. It should be emphasized, apart from the relative uncertainty in the vertical scale, that there is no noticeable difference in the spectrum shape among the spectra shown in Fig. 2 at electron energies above 2 keV, as can be seen by shifting them vertically. This indicates that the spectrum shape is determined by the ion velocity only.

The Z_1^2-scaling behavior of the electron yield for a given target and for ions of equal velocity has been discussed previously,[10] using a perturbation treatment for ion-induced ionizations (semiclassical approximation model). This treatment, however, is not applicable to the case of heavy Si or Cl ions,[12] but, the Z_1^2 scaling has a more general basis in the present case. The measured keV electrons are produced only by large energy transfers from ions to electrons through binary close-encounter processes. Of course, the detected electron energies are degraded by inelastic scatterings suffered along their outgoing path. Such close-impact processes can be reasonably well treated by the binary-encounter approximation (BEA) in which the ionization event is described as a classical encounter between a projectile and a free electron, whose initial velocity distribution is obtained from the target electronic wave function.[13] In the BEA model, the ionization probability $P(b)$ for a given target atom at an impact parameter b is written in the form

$$P(b)=Z_1^2 f(b,v), \qquad (1)$$

where v is the ion's velocity and $f(b,v)$ is the ionization probability for protons with the same velocity.[14] It follows from Eq. (1) that for ions of equal velocity the number of electrons recoiled with a given momentum is proportional to Z_1^2. The Z_1^2-scaling behavior shown in Fig. 1 confirms that the electrons stem from binary collisions with the projectiles. Actually, electron yields in accordance with the binary collision model has been measured in a forward direction using gas targets.[15,16].

Figure 3 shows similar results for 3.75-MeV/amu 0 and S ions incident on GaAs targets, also confirming the Z_1^2-scaling behavior. In Fig. 3 no appreciable difference in the random electron yield above 2 keV is seen for an oblique ($\theta=45°$) and a perpendicular ($\theta=90°$) incidence beam direction. Such independence of the sample mounting with respect to the beam direction is characteristic of the 180° detection of the backscattered, but otherwise straightly moving, high-energy electrons. This is so because, for straightly moving electrons, the reduction of the yield under oblique incidence (proportional to sin θ)

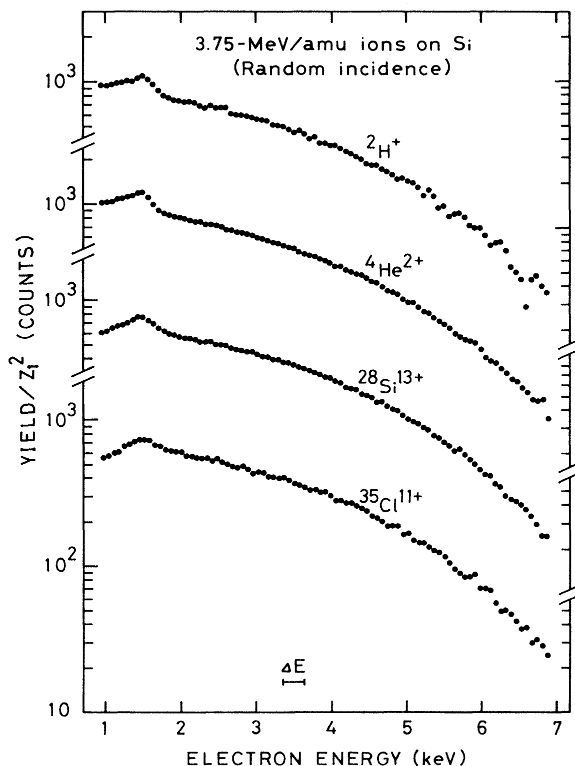

FIG. 2. Energy spectra of secondary electrons induced by 3.75-MeV/amu deuterons, He, Si, and Cl ions, measured for random incidence on a Si crystal. The electron yields are divided by the square of the ion's atomic number, Z_1, and normalized to the same number of incident ions. The spectrometer's energy resolution $\triangle E$, which is proportional to the electron energy, is shown representatively at 3.5 keV. The peaks near 1.6 keV are due to Si K-shell Auger electrons.

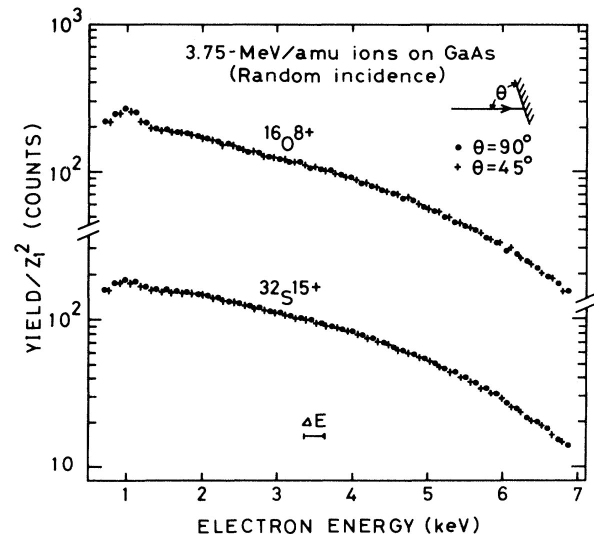

FIG. 3. Energy spectra of secondary electrons induced by 3.75-MeV/amu O and S ions, measured for 45° and 90° random incidence on a GaAs crystal. The normalization of the yields is similar to that of Fig. 2. The peaks near 1 keV are due to *L*-shell Auger electrons of Ga and As.

is canceled by the increased number of electrons produced in a given layer by the incident beam (proportional to $1/\sin\theta$). It should be noted that a small difference of the electron yields near or below 1 keV is seen in Fig. 3 between the oblique and perpendicular cases. This is due to the disturbed electron trajectories going from the sample to the entrance of the electron's guide pipe (Fig. 1) for the case of $\theta=45°$, for which the electric field of the suppressor plate (-200 V) surrounding the sample has a component perpendicular to the spectrometer's entrance axis. This disturbance effect became noticeable for the yield below about 2 keV when the suppressor voltage was lower than about -400V.

B. Localization of close-encounter recoils near the surface

Figure 4 shows energy spectra of secondary electrons for a GaAs crystal preamorphized with 2-keV Ar^+ to a beam dose of about 10^{15} cm^{-2}. The spectra are measured using 60-MeV O^{8+} ions under ⟨100⟩ channeling conditions. As compared to the undamaged crystal the electron yields below 7 keV for the GaAs ⟨100⟩ are enhanced by 27%. This enhancement, a monitor for the damage production, remained constant for further bombardment of Ar^+ up to the beam dose of about 5 times higher. The projected range of 2-keV Ar in GaAs is about 60 Å according to the LSS calculations.[17] Thus, the 27% increase in the electron yield arises from the heavily damaged surface region whose thickness is roughly equal to $60\cos45°\simeq42$ Å. (The direction of incidence of the Ar beam is 45°.)

The keV electrons recoiled near the surface in a forward direction can only be detected if they are backscattered somewhere in the target. Consequently, they suffer energy loss during the passage into the interior of the crystal and back to the surface. For the random case, the effect of energy loss of electrons on the spectra is stronger than for the channeling case; for there are also target electrons that are recoiled in deeper regions, and therefore, experience even more inelastic scatterings along their path to the surface. In Fig. 4, as can be clearly seen by a vertical shift of the spectra for electron energies less than about 8 keV, the ⟨100⟩ spectra before and after the bombardment have the same shape, while the random spectrum has a smaller slope than the aligned spectra. The separation between the spectra of the damaged and the undamaged crystal is slightly larger at electron energies above the binary-peak energy of 8.2 keV. The similarity between the spectrum contribution of the damaged layer and that of the undamaged crystal indicates that under channeling incidence conditions the large majority of the recoils are produced in the surface region of the crystal. Therefore, Fig. 4 provides evidence for the localization of the close-encounter recoils near the surface under channeling incidence conditions.

Intermediate spectrum shapes are observed for weak channeling conditions. Figure 5 shows the electron spectra for GaAs ⟨100⟩ axial, (110) planar, (100) planar, and random incidences of 60-MeV O^{8+}, normalized to the spectrum for the strongest ⟨110⟩ channeling case. As seen in Fig. 5, the normalized electron yields for ⟨100⟩ and (110) cases are nearly constant above about 3 keV: the spectrum shape is the same as for the ⟨110⟩ case. The normalized electron yield for the weaker (100) channeling condition, however, gradually increases above 3 keV. This indicates a larger contribution of energy-degraded electrons, compared with the ⟨110⟩ case. Thus, more electrons are produced in deeper regions of the solid. It should be noted that above 6 keV the normalized yield for the random case increases up to about

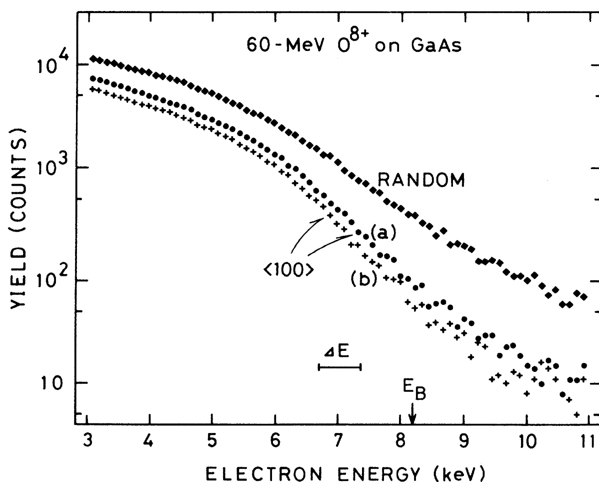

FIG. 4. Energy spectra of secondary electrons induced by 60-MeV O^{8+} for ⟨100⟩ incidence on GaAs before (b), and after (a) bombarding with 2-keV Ar^+ to a beam dose of about 10^{15} cm^{-2}. E_B indicates the binary-peak energy (see text).

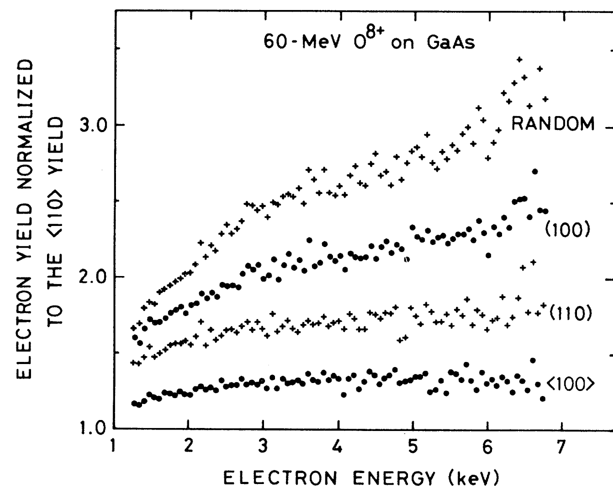

FIG. 5. Secondary electron yields for GaAs ⟨100⟩, (110), (100), and random incidences of 60-MeV O^{8+}, relative to the yield for the ⟨110⟩ case.

10, the inverse of the ratio of the ⟨110⟩ channeling to random yield for inner-shell electrons, see also Fig. 4.

C. Effective target thickness for channeling incidence

To evaluate the thickness of the damaged GaAs layer, the depth dependence of the probability for a close encounter between an ion and a target electron under channeling incidence conditions has been calculated by computer simulations.

The method of simulations is essentially similar to those commonly used in ion-beam analyses of surface structures.[18,6] The simulations are of the so-called multistring type. The probability for a close encounter with an electron of a target atom, written as a function of the impact parameter, is assumed to be simply proportional to the two-dimensional electron density. The density is obtained by projecting the electron distribution of the atom onto a plane perpendicular to the channel direction. The electron distribution used was obtained from the atomic potential given by the Molière approximation to the Thomas-Fermi potential,[11] by applying the Poisson equation. The Molière potential was used to calculate the trajectories of the incident O^{8+} ions in GaAs (the Thomas-Fermi screening length is 0.147 Å). The two-dimensional root-mean-square thermal vibration amplitude of atoms in GaAs was taken to be 0.13 Å at room temperature, since this value enables reasonable analysis of surface peaks observed in ion backscattering spectra.[19] We have also calculated the close-encounter probability for typical inner-shell electrons in GaAs, i.e., for *L*-shell electrons. In the simulations, the distribution of the *L*-shell electrons in Ga and As was replaced in a good approximation by that in Ge, obtained from numerical tables for atomic wave functions given by Fischer.[20]

Figure 6 shows the calculated encounter probabilities, normalized to those for the surface layer, for 60-MeV O ions incident in the ⟨110⟩ and ⟨100⟩ axial directions of GaAs. As seen in Fig. 6, the encounter probabilities for all electrons decrease gradually with increasing depth because of the weak shadowing effect for the outer-shell electrons of the atoms. Consequently, it is difficult to identify a fully shadowed region where the close-encounter recoils become negligibly small. For *L*-shell electrons, however, the region below a depth of about 200 Å can be regarded as fully shadowed. For a depth beyond 200 Å, the second approach of the ions to the atomic rows causes only a negligible increase of the encounter probability for *L*-shell electrons. By integrating the calculated probability from the surface to the depth of 200 Å, the effective target thickness for localized close-encounter recoils with *L*-shell electrons is obtained: 52 and 63 Å for ⟨110⟩ and ⟨100⟩, respectively.

In Fig. 4, the electron yields above the binary-peak energy (8.2 keV) result from scattered inner-shell electrons only, for which the effective target thickness is known. By using the value of 63 Å for the ⟨100⟩ case, we can

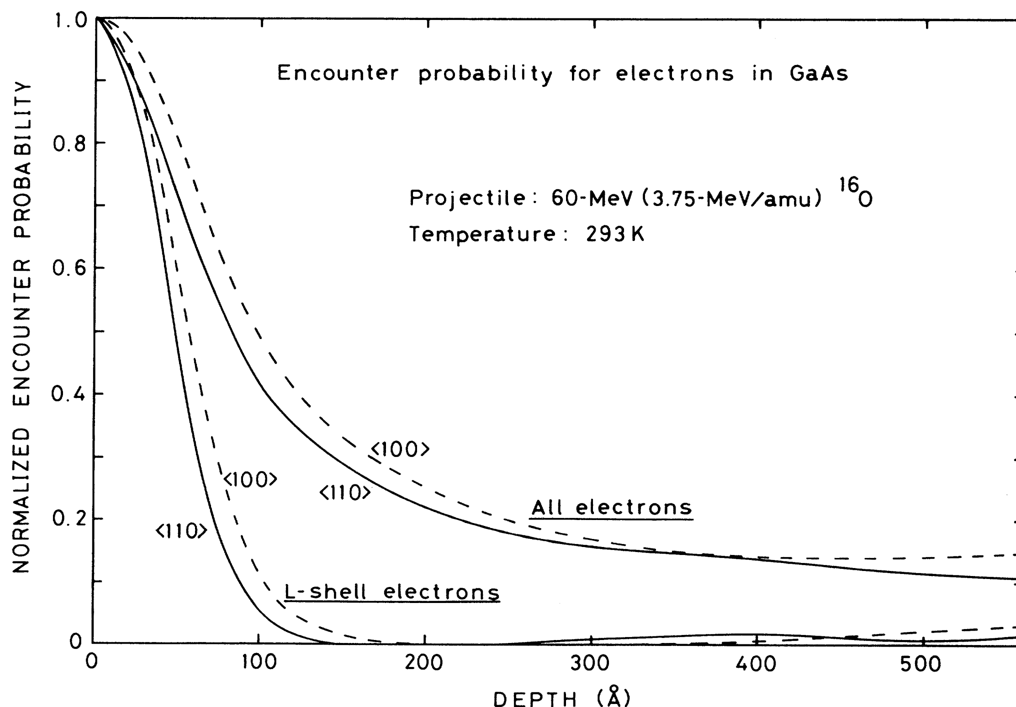

FIG. 6. Calculated encounter probabilities for all and for *L*-shell electrons in GaAs for ⟨110⟩ and ⟨100⟩ incidence of 60-MeV O ions, normalized to the probability at the surface.

determine the thickness of the damaged layer by assuming that this layer is amorphous. Since the K-shells for GaAs have high binding energies (about 10 keV), they are hardly ionized by the ions used here and the measured electron yields result predominantly from scattered L-shell electrons. In our experimental conditions, dechanneling caused by the damaged layer is negligibly small so that the effective target thickness for the damaged GaAs is the sum of the thickness of the damaged layer and the effective target thickness for undamaged GaAs. In fact, this has been confirmed by the simulation results, shown in Fig. 7, for the encounter probabilities for amorphous overlayers of 56.5 and 113 Å thick (10 and 20 times the ⟨100⟩ interatomic distance, respectively). Since the average ⟨100⟩ yield for the damaged GaAs between 8.2 and 10 keV is increased by 57%, the thickness of the damaged layer is calculated to be $0.57\times63=36$ Å. The uncertainty in the value is about ±4 Å. Considering the crudeness of our model, the calculated thickness seems reasonable: only 14% smaller than the thickness of 42 Å estimated in Sec. III B.

The relative increase in spectrum yield caused by the 36-Å thick amorphous layer can be used to determine the effective target thickness for channeling incidence at all energies, also below E_B where the partially shadowed outer-shell electrons contribute to the spectrum yield too. Since the ⟨100⟩ electron yield at 5 keV is enhanced by 27% by the 36-Å thick damaged layer, the effective target thickness at 5 keV for ⟨100⟩ incidence on the nondamaged GaAs crystal is calculated to be $36/0.27=133$ Å. It is worthwhile to note that at a depth of 307 Å the integrated probability for all electrons amounts to 133 Å. Thus, although recoils are also produced deeper than 307 Å below the surface, they hardly contribute to the detected yield.

D. Effective target thickness for random incidence

For random incidence conditions, the close-encounter collisions of ions with target electrons occur over almost the whole range of the ions in the crystal. Most of the electrons are recoiled in a forward direction and backscattering is necessary before escape to the vacuum is possible. Nevertheless, the deeper the electrons are recoiled, the larger is, on the average, the energy loss before escape. If the depth of recoil is too large, the electrons will lose so much energy that their number is negligible compared to the much larger number of electrons detected with the same energy but recoiled closer to the surface with lower initial energy. Therefore, although electrons are recoiled in a very wide region of the solid, only a finite layer near the surface contributes to the spectrum yield. Consequently, for each energy an effective target thickness, t_r, for random incidence can be defined: t_r is the thickness of a target resulting in the same spectrum yield, for the hypothetical case that the electrons do not suffer any energy loss.

The value of t_r can be calculated by using the effective target thickness for channeling incidence. At 9 keV (above the binary-peak energy) t_r for GaAs is calculated

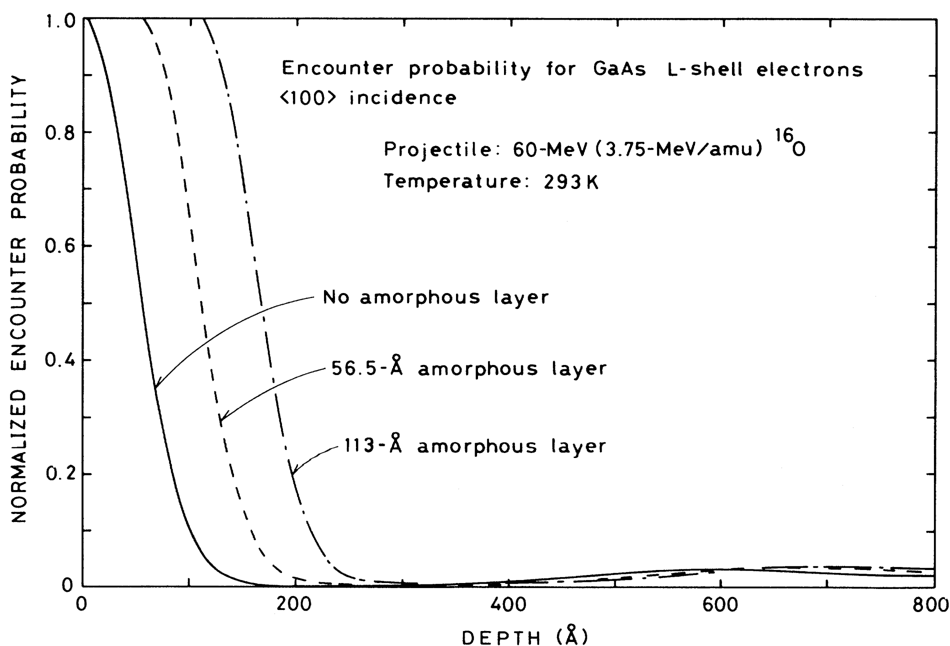

FIG. 7. Calculated encounter probabilities for L-shell electrons in GaAs for ⟨100⟩ incidence of 60-MeV O ions, assuming 56.5- and 113-Å (10 and 20 times the interatomic distance, respectively) amorphized surface layers. In the simulations, the lateral positions of the first 10 or 20 atoms in the ⟨110⟩ row were randomly distributed within the ⟨100⟩ channel. The result for no amorphous layer is also shown for comparison.

to be 63 Å (from simulations) divided by the ratio of the ⟨110⟩ channeling to random yield for undamaged GaAs: $t_r = 63/0.14 = 450$ Å. Below the binary-peak energy, the effective target thickness for channeling cannot be calculated using simulations (Sec. III C), since outer-shell electrons, which are not fully shadowed, contribute to the electron yield as well. The experimental effective target thickness at 5 keV for channeling is 133 Å. The value is obtained via the spectrum of the damaged crystal, as shown in Sec. III C. Since for undamaged GaAs the ratio of the ⟨100⟩ to random electron yield at 5 keV is 0.46, see Fig. 4, t_r at 5 keV is obtained as $133/0.46 = 290$ Å. This value is in good agreement with the maximum depth of 307 Å contributing to the electron yield at 5 keV that follows from the analysis of the channeling spectrum, see Sec. III C.

IV. CONCLUDING REMARKS

The observed Z_1^2-scaling behavior of keV electron yields for equal-velocity ions of various species in the MeV/amu range confirms the simple binary collision character of the interaction of the ions with target electrons.

The observed increase in the electron yield after damaging a surface region of a GaAs crystal supports the concept of an effective target thickness for channeling incidences. Such a concept simplifies the analysis of experimental data of the shadowing effect on secondary electron emission, as will be demonstrated elsewhere.[21]

ACKNOWLEDGMENTS

We thank Dr. N. Stolterfoht for valuable comments on this work. We are also grateful to the staff member of Tandem Accelerator Center, University of Tsukuba for their assistance in the experiments. An early stage of this work was supported in part by a Grant-in-Aid from the Ministry of Education, Science, and Culture.

*Present address: ULVAC Corporation, Kanagawa 253, Japan.

[1] G. D. Magnuson and C. E. Carlston, Phys. Rev. **129**, 2409 (1963).

[2] N. Colombie, B. Fagot, and C. Fert, Radiat. Eff. **2**, 31 (1969).

[3] B. A. Brushilovsky and V. A. Molchanov, Radiat. Eff. **23**, 131 (1974).

[4] N. Benazeth, Nucl. Instrum. Methods **194**, 405 (1982).

[5] J. R. MacDonald, L. C. Feldman, P. J. Silverman, J. A. Davies, K. Griffiths, T. E. Jackman, P. R. Norton, and W. N. Unertl, Nucl. Instrum. Methods **218**, 765 (1983).

[6] H. Kudo, D. Schneider, E. P. Kanter, P. W. Arcuni, and E. A. Johnson, Phys. Rev. B **30**, 4899 (1984).

[7] H. Kudo, K. Murakami, K. Takita, K. Masuda, S. Seki, K. Shima, H. Itoh, and T. Ipposhi, Jpn. J. Appl. Phys. **24**, 1440 (1985).

[8] H. Kudo, K. Shima, K. Takita, K. Masuda, K. Murakami, H. Itoh, T. Ipposhi, and S. Seki, Jpn. J. Appl. Phys. **27**, 1751 (1986).

[9] L. Wong, P. F. A. Alkemade, W. N. Lennard, and I. V. Mitchell, Nucl. Instrum. Methods B **45**, 637 (1990).

[10] H. Kudo, K. Shima, S. Seki, K. Takita, K. Masuda, K. Murakami and T. Ipposhi, Phys. Rev. B **38**, 44 (1988).

[11] D. S. Gemmell, Rev. Mod. Phys. **46**, 129 (1974).

[12] J. M. Hansteen, O. M. Johnsen, and L. Kocbach, At. Data Nucl. Data Tables **15**, 305 (1975).

[13] C. L. Cocke, in *Methods of Experimental Physics,* edited by L. Marton and C. Marton (Academic, New York, 1980), Vol. 17, Chap. 7.

[14] J. H. McGuire, Phys. Rev. A **9**, 286 (1974).

[15] N. Stolterfoht, in *Topics in Current Physics* (Springer-Verlag, Berlin, 1978), Vol. 5, p. 155.

[16] D. H. Lee, P. Richard, T. J. M. Zouros, J. M. Sanders, J. L. Shinpaugh, and H. Hidmi, Phys. Rev. A **41**, 4816 (1990).

[17] J. Lindhard, M. Scharff, and H. E. Schiøtt, K. Dan. Vidensk. Selsk. Mat. Fys. Medd. **33**, No. 14 (1963).

[18] L. C. Feldman, J. W. Mayer, and S. T. Picraux, *Material Analysis by Ion Channeling* (Academic, New York, 1982).

[19] T. Narusawa, K. L. I. Kobayashi, and H. Nakashima, Jpn. J. Appl. Phys. **24**, L98 (1985).

[20] C. Froese Fischer, At. Data **4**, 301 (1972).

[21] H. Kudo, K. Shima, S. Seki, and T. Ishihara, following paper, Phys. Rev. B **43**, 12 736 (1991).